Synergistic Effect of Autophagy Inhibitor Si-beclin1 Combined With the Doxorubicin Nano-delivery System Against Advanced Prostate Cancer

Chuling Hu
Second Military Medical University
Fenfen Gu
Second Military Medical University First Hospital: Changhai Hospital
Yuan Gao
Fudan University
Chunai Gong
Second Military Medical University First Hospital: Changhai Hospital
Qingming Xia
Second Military Medical University
Shen Gao (liullk@126.com)
Department of Pharmaceutics, Changhai Hospital, Second Military Medical University, Shanghai 200433, China https://orcid.org/0000-0002-5125-1606

Research

Keywords: autophagy, si-Beclin1, chemotherapy, nanotechnology, prostate cancer

DOI: https://doi.org/10.21203/rs.3.rs-128663/v1

Abstract

Apoptosis tolerance is an important mechanism of tumor resistance in tumor therapy. Autophagy can prevent apoptosis induced by antitumor drugs and promote tumor resistance. The purpose of the presentn study was to improve the sensitivity of chemotherapeutic drugs and enhance the efficacy by inhibiting autophagy. In the present study, hydrophobic doxorubicin-hydrazone-caproyl-maleimide (DOX-EMCH) and autophagy-inhibitory si-Beclin1 were simultaneously delivered via the amphiphilic peptide micelle system(Co-MPs) using ploy(L-arginine)-poly(L-histidine)-DOX-EMCH as the copolymer building unit. It was found that the constructed micelle system promoted the escape of si-Beclin1 from endosomes and the release of DOX into the nucleus and the Co-MPs exhibited 2.7–fold higher cytotoxicity and apoptosis, in PC3 cells than DOX treatment alone did, which demonstrates the si-Beclin1 inhibited the autophagy activity of prostate cancer (PCa) cells by targeting the type III PI3K pathway and improve the sensitivity to the chemotherapy drug DOX. In addition, the peptide micelles successfully targeted DOX and si-Beclin1 passively to the tumor tissue. Compared with DOX or si-Beclin1 treatment alone, the Co-MPs showed a 3.4-fold greater tumor inhibition in vivo, which demonstrated a synergistic anti-proliferative effect in vivo. Our results suggest that the Co-MPs developed in this study may prove to be a promising combination method to provide autophagy inhibition and chemotherapy in cancer treatment, especially for PCa.

1. Background

The rising incidence of prostate cancer (PCa) has seriously endangered human health in men. According to the 2019 data from the communications authority (CA), PCa is the leading cause of cancer-related death in men in the United States [1]. Endocrine therapy is the mainstay of treatment for advanced PCa. However, most patients gradually converted to hormone refractory PCs after a median duration of 14–30 months and died of steroid resistant tumors and distant metastasis[2–4]. It is therefore a challenging task to treat PCa effectively in clinical practice. The focus of current research with Doxorubicin (DOX)-based combination therapy is a first-line chemotherapy after complete failure of endocrine therapy[5–7], but the toxic and adverse effects of systemic chemotherapy, exogenous and endogenous drug resistance often lead to the failure of chemotherapy[8–10]. Some studies [11–14] suggested that it was probably caused by the abnormal increase in autophagy activity in PCa cells.

Autophagy is a process of cell self-degradation, which plays an important role in the regulation of metabolic stress and maintenance of genome integrity and stability of the internal environment. Autophagy is closely associated with cancer and is bidirectional to tumor cells. Autophagy can prevent apoptosis induced by antitumor drugs, and promote tumor resistance [15–17].Some studies [18–20] reported that treatment with Docetaxel significantly up-regulated autophagy in lung cancer, and that autophagy inhibitors could regulate the autophagic activity, thus improving the efficacy of Docetaxel, suggesting that inhibition of autophagy to promote the sensitivity of chemotherapeutic drugs may also be an alternative treatment for PCa.

Beclin1 gene, also known as BECN1, is a homologue of yeast ATG6, also known as mammalian autophagy specific gene. The Beclin1 gene regulates other ATG proteins, localization of autophagy precursors andautophagy activity mainly by forming a complex with III PI3K[21–23]. It has been demonstrated that up-regulation of Beclin1 expression in mammals can stimulate autophagy[24, 25]. Currently, Beclin1 has been identified as a novel candidate tumor suppressor gene. As reported[26], deletion mutation of BECN1 gene in ovarian cancer, breast cancer and PCa is as high as 40–75%. They found that the expression level of Beclin1 gene was increased significantly in A549 cells treated with paclitaxel, hindering the final cell death. But administration of autophagy inhibitors or small interfering RNA could obviously promote cell apoptosis[27]. Si-Beclin1 was used to down-regulate the expression of Beclin1 and inhibit the activity of autophagy in PCa by targeting III PI3K pathway, and the result showed that it could enhance the sensitivity of the drug, which further suggests that Beclin1 siRNA may be a novel approach for the treatment of PCa[28]. But whether co-delivery of Beclin1 siRNA and common chemotherapy drugs to the tumor tissue could improve the sensitivity of advanced PCa to DOX chemotherapy needs to be verified. The aim of the present study was to synthesize a pH sensitive polymer DOX–$H_3R_6$and use R_6 (Arginine 6) as an intracellular delivery vector to see whether they could work synergically to compress RNA by electrostatic interaction[29–31]. Histidine can help nanomicelles escape from the endosome through the proton sponge effect [32, 33]. DOX-EMCH is a 6-maleimide acetylhydrazone derivative of doxorubicin. DOX was conjugated with H_3CR_6C through amide bond. DOX-H_3CR_6C was cross-linked by cysteine(DOX- H_3R6ss). The amide bond could crack in the glutathione-reducing conditions present in tumor cells, releasing the drug [34, 35]. To form the co-delivery nanomicelle (Co-MPs), DOX- H3R6ss assembled into a nanomicelle, in which DOX was encapsulated in the hydrophobic core, and si-Beclin1 was condensed on the hydrophilic layer (Scheme 1). The size, zeta potential, cellular uptake, autophagy inhibition, cytotoxicity and apoptosis were determined, and the vivo distribution and anti-tumor effect were investigatedin a PCa xenograft nude model. We hypothesized that the co-delivery of DOX and si-Beclin1 could effectively inhibit autophagy, enhance the cytotoxicity of chemotherapy, promote cell apoptosis, and inhibit the growth of the cancer xenograft, hoping that the co-delivery system has potential to treat hormone refractory PCa.

2. Results

2.1 Preparation and characterization of DOX -conjugated micelles

The size, zeta potential, drug loading and drug encapsulation efficiency of micelle are investigated. DOX was conjugated into the micelles through hydrophobic interactions. As shown in Fig. 2A, B, with the increase of the N/P ratio,the particle size decreased and the potential increased. When the N/P ratio was 40, the mean particle size was 129.9 ± 2.5 nm, and the polydispersity index (PDI) was 0.086 ± 0.820. The Zeta potential was 25.8 ± 1.65 mV. The reasonable size and zeta potential of Co-MPs make them suitable for systematic administration through the EPR effect of the delivery system[36, 37]. The TEM image of Co-MPs showed a spherical shape and a good dispersion (Fig. 2C).

The condensation ability of the complexes was determined by agarose gel electrophoresis. As shown in Fig. 2D, with the N/P ratio increasing from 0.5 to 20, the condensing ability of DOX- conjugated micelles was enhanced gradually. When the N/P ratio was greater than 10, the si-Beclin1 was completely condensed, indicating that the compression ability of DOX- conjugated micelles was improved by electrostatic interaction[38]. To confirm this finding, DTT, a reducing agent, was used to break this disulfide bond. As shown in Fig. 2D, the Co-MPs showed a weaker si-Beclin1 binding affinity in the presence of DTT because of the depolymerization of Co-Mps. Based on the above results, we hypothesized that the broken of inter-molecular disulfide bond can release DOX and si-Beclin1 by reducing the condition in the cytoplasm, thus reducing the affinity of CO-MPs. This reductive sensitive drug delivery system remain stable extracellularly but not stable in the cytoplasm, which can maintain effective release.

2.2 Release at different pHs of DOX

The DOX release profiles of Co-MPs were investigated at pH5.5 and pH 7.4 at 37℃, respectively. As shownin Fig. 2E, the release of DOX from the micelles was pH-sensitive. For example, DOX release from Co-MPs reached 78.9% at pH 5.5 but only 54.8% at pH 7.4 ($P < 0.01$) when observed for 48 h, which is most likely due to the release of the DOX from the disulfide bond under acidic conditions and protonation of the histidine within the structure of the micelles at endolysosomal pH (about 5.0)[39, 40]. The proton sponge effect of histidine can destroy the internal structure of micelles, thereby promoting the release of DOX[41].

2.3 Cellular uptake

Knowing that effective cellular uptake is essential for drug delivery[42], we labeled si-Beclin1with FAM probe, and incubated DOX, DOX-MPs and Co-MPs with PC3 cells for 4 h. The positive cells were quantitatively assessed by flow cytometry after 4-h incubation. As shown in Fig. 3A, B, the fluorescent signal of FAM increased with the increase of the N/P ratio, and when the N/P ratio was 80, the number of positive FAM cells was 1.79-fold and 1.32-fold as high as that at an N/P ratio of 20 and 40($p < 0.05$). The uptake of DOX in PC3 cells showed a dose-dependent manner, and the positive cells at 0.5 μg/ml, 1 μg/ml and 2 μg/ml accounted for 45.57%, 54.11% and 88.66% respectively. But the DOX-MPs had higher cellular uptake at a low concentration. When the concentration was 0.5 μg/ml, the percentage of positive cells was 93.01% (Fig. 3C, D). It was shown that doxorubicin modified by the membrane penetrating peptide was easier to enter the cell after being made into micelles. It is noteworthy that Co-MPs showed the optimal gene uptake efficiency at an N/P ratio of 40.

To observe the intercellular location of DOX, DOX-MPs and Co-MPs, PC3 cells were observed under a confocal laser scanning microscope (CLSM). DAPI (4',6-diamidino-2-phenylindole) was used to stain the nucleus. Figure 3E shows the intracellular distribution of the micelle in PC3 cells for 4 h after transfection. In the free DOX, red fluorescence was distributed in the nucleus and cytoplasm in coincidence with blue fluorescence. In the DOX-MPs group, red fluorescence was also distributed in the nucleus and cytoplasm, and the fluorescence intensity was brighter than that of the simple group, indicating that the DOX could

enter the nucleus to play the cytotoxic effect. In Co-MPs, the red fluorescence and green fluorescence were partly distributed in the nucleus and cytoplasm, indicating that DOX and si-Beclin1 were successfully transported into cells by nanomicelles, and FAM-si-Beclin1 successfully escaped from the endosome and entered the nucleus[43, 44]. These results suggest that the co-delivery system could promote endosomal escape, and carry the genetic and chemotherapeutic drug into the nucleus. This finding was in good agreement with the flow cytometry data.

2.4 In vitro evaluation of autophagy inhibition

To evaluate the autophagy inhibition capability of Co-MPs in PC3 cells, flow cytometry and confocal microscopy were used to monitor autophagy. As shown in Fig. 4A, the autophagy level of free DOX was significantly higher than that in DOX-MPs and Co-MPs groups when the concentration of DOX was 0.5 μg/mL and si-Beclin1 was 100 nM. The percentage of autophagy-postive cells in Co-MPs group was lower than that in DOX group (6.77% vs18.00, $P < 0.05$), indicating that si-Beclin1 could be effectively co-delivered by Co-MPs and inhibited autophagy caused by nanomaterials.

In addition to observing autophagosomes, the aggregation of fluorescent spots in autophagic flux observed by confocal microscopy was also used. Tandem fluorescent-tagged LC3(mRFP-EGFP-LC3) was used to monitor autophagic flux based on the different sensitivities of EGFP and mRFP fluorescent proteins to acidic pH[45]. The weakening of GFP could indicate the fusion of lysosomes and autophagosomes to form autophagolysosomes. At this time, GFP fluorescence was quenched and only red fluorescence was displayed. As shown in Fig. 4B, the fluorescence intensity of the autophagy marker protein LC3II increasedgradually in GFP-labeled DOX group as compared with the control group, and punctate red fluorescence distribution was also increased, suggesting that autophagy PC3 cells were activated. The red fluorescence intensity in DOX-MPs group was decreased as compared with that in DOX group, and the fluorescence intensity in Co-MPs group was the weakest, indicating that autophagy in the total load group with the expression of si-Beclin1 was inhibited, thus reducing the DOX-enhanced autophagy.

In addition, the dynamic process of autophagy was observed by TEM. The presence of autophagic vacuoles in the cytoplasm indicates the emergence of autophagy[46]. Figure 4C shows the treatment of the cells with si-Beclin1, DOX, DOX-MPs and Co-MPs(DOX:0.5 μg/mL and si-Beclin1: 100 nM). In the control group, the cell structure was clear, the nuclear membrane was smooth, and the cytoplasmic organelles were rich. But the crista of mitochondria in DOX-MPs and DOX groups was ruptured, swollen and denatured, and the number of autophagosomes was increased significantly as compared with si-Beclin1 and Co-MPs groups, indicating that DOX was able to induce more autophagicvacuoles, and less autophagy was produced in nanoparticles of DOX.

The result of LC3II/I qRT-PCR analysis showed that LC3II/I proteins was downregulated by 41.3% and 10.3% in the Co-MPs group compared with that in the DOX and DOX-MPs(Fig. 4D). Furthermore, to explore the role of beclin1 in regulating doxorubicin-induced autophagy, the expression levels of beclin1, LC3 and P62 was detected by Western blot. Compared with the control group, DOX treatment induced a

significant increase in the expression of the autophagy marker protein LC3II and a significant decrease in the expression of p62 protein(Fig. 4D). In addition, the expression of LC3II was weak in Co-MPs group, and p62 accumulated in the Co-MPs, indicating that DOX could induce PC3 cell autophagy, and wrapping of si-Beclin1 nanoparticles could reduce the incidence of autophagy.

2.5 Cell viability assay

The cytotoxicity in PC3 cells of different groups was investigated. Figure 5A, B show the cell viability after treatment with free DOX, DOX-MPs and Co-MPs at the concentration of DOX of 0 μg/mL to 2 μg/mL and si-Beclin1 concentration of 100 nM for 24 and 48 h. The proliferation of PC3 cells was inhibited in the three groups in a concentration-dependent manner. CCK-8 assay demonstrated that the IC50 value in PC3 cells at 48 h was 0.95 μg/mL,0.70 μg/mL and 0.45 μg/mL in free DOX, DOX-MPs, and Co-MPs group respectively. The IC50 value in Co-MPs group was about 2.1-fold lower than that in free DOX group ($P < 0.05$), indicating that co-delivery of DOX and si-Beclin1 could accelerated the intracellular DOX release and improved the endo/lysosomal escape and the release of si-Beclin1, making the Co-MPs an efficient co-delivery system with good synergy between DOX and si-beclin1, and enhanced the cytotoxic of DOX.

2.6 Cell apoptosis

Figure.5C shows PC3 cell apoptosis in each group. No significant apoptosis was observed in PC3 cells exposed to si-Beclin1 after 48-h treatment. Compared with the control group, cell apoptosis was reduced by 19.87% in DOX-MPs group, which was approximately 1.35-fold higher than that in free DOX group(14.67%).In Co-MPs group, cell apoptosis was reduced by 39.77%, which was approximately 2.0- and 2.7-fold higher than that in DOX-MPs group and free DOX group. These results suggest that Co-MPs could silence the si-Beclin1 gene and inhibit the autophagy caused by the chemotherapy drug doxorubicin.

2.7 In vivo distribution

The investigation of in vivo distribution is essential for the evaluation of safety and effectiveness of nano-micellar delivery[47]. Doxorubicin has its own fluorescence, which can be used as an indicator to reduce the interference of animal autofluorescence[48, 49]. The tumors and major organs were excised to investigate the biodistribution of DOX and DOX-PMs. As shown in Fig. 6A, the tumors and the anatomical organs were scanned at 24 h post-administration, and images were obtained. A fluorescence signal was observed in the liver, lung, kidney, and tumor in the naked DOX. In DOX-MPs group, significant fluorescence accumulation was observed in the tumor site as a result of the EPR effect by MPs due to their nanosize. The quantitative analysis indicated that the signal intensity of DOX in the tumor tissue of DOX-MPs group was 5-fold higher than that in free DOX group ($P < 0.01$), and 3.2-fold lower than that in the liver of free DOX group ($P < 0.01$). This was due to the EPR effect and the avoidance of the reticuloendothelial system (RES) by the nanosize of the micelles. Above all, these results indicate that DHRss micells have the ability of high efficient drug delivery into tumor tissues via the EPR effect[50, 51].

2.8 In vivo antitumor effect

The in vivo antitumor effect of Co-MPs and the synergistic effects of DOX and si-Beclin1 were investigated in PC3 human androgen-independent prostate tumor-bearing nude mice. The tumor volume and body weight of the nude mice were monitored at regular intervals. As shown in Fig. 6B, no inhibitory effect on tumor growth was observed in the normal saline group andsi-Beclin1 group. The tumor volume was the smallest and the inhibitory effect was the most obvious in Co-MPs group as compared with the other groups ($P < 0.01$). The tumors were 4.8-,3.4- and 2.1-flod smaller in Co-MPs group than those in the groups treated with si-beclin1, DOX, and DOX-MPs, respectively at day 21, which confirms the synergistic effect of DOX and si-Beclin1 against PC3 solid tumors in vivo. There was also confirmed by the difference in the average weight of isolated tumors at day 21(Fig. 6C)($p < 0.05$). This is consistent with the antitumor effect in vitro.

The safety of Co-MPs was evaluated by body weight changes before and after administration of DOX in nude mice[52]. As shown in Fig. 6D, the body weight of the nude mice in DOX group increased slowly and then decreased in the whole process, indicating that DOX-MPs, si-Beclin1 and Co-MPs did not induce significant systemic toxicity during the experimental period. However, significant weight loss was observed in free DOX group due to the systemic toxicity of DOX ($p < 0.01$)[53].

2.9 TUNEL and immunohistochemistry analysis

TUNEL staining assay was used to determine whether the Co-MPs could induce the cancer cell apoptosis which was a key factor in the inhibition of cell proliferation. As shown in Fig. 7A, an increased brown staining could be obtained in the group treated with Co-MPs. Thus, the anti-proliferative mechanism of Co-MPs was identified to associate with the induction of cell apoptosis. The immunohistochemical result showed that Co-MPs significantly inhibited the expression of LC3 protein, which was represented by the reduction of Ki67 (Fig. 7B), a key points in cell proliferation. The above results indicate that co-loaded micelles enhanced the anti-tumor activity of chemotherapeutics and were related to the inhibition of autophagy of tumor cells.

Histological analysis

Histological study was performed to further evaluate the in vivo antitumor safety. As shown in Fig. 7C, the HE staining results of tissues and organs showed that in DOX group, the myocardial cells were damaged, the myocardial fibers were ruptured, and the intermuscular space was widened. But no significant organ toxicity was observed in si-Beclin1, DOX-MPs and Co-MPs groups. The results showed that DOX delivered by Co-MPs has remarkably reduced cardiotoxicity compared with free DOX.

2.10 Evaluation of in vivo autophagy inhibition

The process of autophagy was observed in vivo by TEM. The presence of autophagic vacuoles in the cytoplasm indicates the emergence of autophagy. As shown in Fig. 7D, the number of autophagosomes in DOX and DOX-MPs groups increased significantly as compared with si-Beclin1 and Co-MPs groups.

This is consistent with the previous in vitro cytology experiments, indicating that inhibiting autophagy gene beclin1 could down-regulate the autophagy level in tumor tissues.

3. Discussion

Autophagy is an important mechanism for cells to adapt to environmental changes, prevent the invasion of pathogenic microorganisms and maintain the stability of internal environment. Autophagy activity changes in a variety of human tumors. Autophagy plays a dual role in promoting and inhibiting tumor development. In case of tumorigenesis, cancer cells confer stress tolerance such as acid environment, chemotherapy, hypoxia and deficiency of nutrition by utilizing autophagy. In some cases, the cancer cells also activate autophagy in response to various chemotherapeutic drugs, which resist cell death and decrease the curative effect [54, 55].

In this study, PC-3 cell line was used as a model to investigate the synergistic efficacy of the combination of chemotherapy and autophagy inhibition by co-delivery nanomicelle. We have successfully synthesized a amphiphilic peptide micelle system for co-delivery of si-beclin1 and DOX, which can effectively silence beclin1 gene suppress DOX-induced autophagy, and consequently showed obvious tumor killing effect. The results of transmission electron microscopy showed that the number of autophagosomes was significantly reduced by co-delivery system. Laser confocal results show that aggregation of mRFP-LC3 spots means the aggregation of autophagic bubbles. Western blot also confirm this conclusion. In addition, the combination of si- Beclin1 and DOX significantly induced apoptosis and necrosis of tumor cells. The antitumor effect of Si Beclin1 and DOX in vivo showed a significant synergistic effect.

Berlin 1, which is homologous with yeast autophagy gene AT96, is a key factor that mediates the localization of other autophagy proteins in preautophagosomes, and participates in the regulation of mammalian autophagy formation. Beclin 1 combined with type III P13K and vps34 to induce autophagy[56]. Therefore, Beclin 1 is an important gene regulating autophagy. In our study, we successfully developed a co-delivery system with good target ability. The results showed this co-delivery system can effectively silence Beclin1gene expression and suppress DOX-induced autophagy, which could underlie its therapeutic antitumor effect and reduce systemic toxicity.

4. Conclusions

In the present study, we demonstrated successful application of self-assembling polypeptide-based cationic micells for co-delivery of si-Beclin1 and the chemotherapeutic drug DOX into androgen-independent prostate cancer cells both in vitro and vivo. Our results show that the synthesized peptide micelles could effectively encapsulate gene drug si-Beclin1 and chemotherapy drug doxorubicin. In vitro experiments showed that peptide micelles could load DOX and si-Beclin1 into PC3 cells, and enhance cell anti-proliferation and apoptosis by inhibiting autophagy caused by DOX. In addition, in vivo experiments showed that peptide micelles could be targeted to the tumor site through the EPR effect, and effectively

inhibit the growth of PC3 xenograft tumors in nude mice. It is expected to become an effective means of combined tumor therapy.

5. Experimental Section

5.1 Materials

All chemicals and organic solvents were of analytical grade. Chemicals and instruments used in this study included Doxorubicin hydrochloride, L-arginine, L-histidine hydrochloride and L-cysteine hydrochloride (Sangon Biotech, Shanghai, China); Beclin1siRNA (CST); Cell Counting Kit-8 (Dojindo Molecular Technologies, Tokyo, Japan); mRFP-EGFP-LC3 (Genomeditech, Shanghai, China); PC3 cells (Institute of Biochemistry and Cell Biology, Shanghai, China); Roswell Park Memorial Institute medium (RMPI 1640), penicillin-streptomycin solution (5 KU/mL) and fetal bovine serum (FBS) (Life Technologies, Grand Island, USA); Gelred (Biotium, CA, USA); Matrigel (BD Biosciences, Spaeks, MD, USA); Annexin V-APC Apoptosis Analysis Kit (eBioscience, CA, USA); Antibodiesagainst Beclin1, P62, LC3I/II, paxillin, anti-Ki67 and β-actin (Cell Signaling Technology); and Autophagy Assay Kit (Sigma-aldrich, California, USA). All animal experiments were performed in accordance with the approval of the ethics committee of the Second Military Medical University(Shanghai, China).

5.2 Cells and cell culture

Human PC3 cells (Institute of Biochemistry and Cell Biology, Shanghai, China) were cultured in RPMI 1640 with 10% FBS and 1% penicillin-streptomycin, and incubated under 5% CO_2 atmosphere at 37℃.

5.3 Plasmid and transfection

mRFP-EGFP-LC3 plasmid was from Addgene. Cells were transiently transfected with the plasmid using lipofectamine 2000 (Invitrogen) according to the manufacture's instructions.

5.4 Synthesis of DHRss

First, a histidine-arginine peptide (CH3CR6, HR) was synthesized using the method of F-moc-solid phase peptide synthesis (SPPS). Second, DOX was coupled to Terminal carboxyl group of HR peptide to obtain DOX-HR (DHR) through condensation reaction. The products were purified by reverse HPLC. Then, the DHR(50 mg) and L-cysteine hydrochloride (0.58 mg) were dissolved in 1.8 mL distilled water (pH 7.0). Then, 0.2 mL 5% hydrogen peroxide was added dropwise to the mixed solutions with stirring and incubated for 12 h. Then, the mixture was dialyzed in water for 12 h and freeze-dried for another 24 h to produce DHRss.

5.5 Preparation of DHRss polymer micelle (DOX-PMs), si-Beclin1 loaded HRss polymer micelle (Co-MPs)

The DOX Conjugated DHRss polymer micelle (DOX-PMs) was prepared using the probe-based ultrasonication technique. DHRss (5 mg) was dissolved in 8 mL distilled water. Then, 2 mL

dichloromethane was injected into the DHRss solution dropwise, followed by ultrasonication at 200W for 1 min in an ice bath using a probe-based sonicator (JY92-IIN, Xinzhi Scientific Co., Ltd., Ningbo, China). Then, the mixed solution was immediately stirred overnight at room temperature to eliminate dichloromethane. Finally, a Millipore (MW = 3000) was used to remove the monomer in the micellar dispersion (Fig. 1). DOX conjugated and si-Beclin1-loaded DHR polymer micelles (Co-PMs) were prepared by adding an appropriate amount of si-Beclin1 to DOX-PMs at N/P = 40, followed by vortexing for 30 s and incubated for 30 min at room temperature before use.

5.6 Complex characterization

5.6.1 Particle size, zeta potential and transmission microscopy (TEM)

The particle size and zeta potential of the DOX-PMs (1 mg/mL) and Co-PMs (N/P = 40, 2 μg/mL siBeclin1) were measured by dynamic light scattering (Zetasizer Nano ZS90, Malvern) at 25 ℃.Co-PMs morphology was examined using a transmission electron microscopy (TEM, Hitachi, Japan) using an acceleration voltage of 75 kV.

5.6.2 Agarose gel electrophoresis

The condensation ability of the complexes was determined by agarose gel electrophoresis. The complexes were prepared at different N/P ratios (0.25-20). After 30-min incubation, the complex (1 μg siBeclin1) was added to the pores of an acetic acid-EDTA buffer and TAE-containing 1% agarose gel. The gel was run at 100V for 30 min. The nucleic acid framework was irradiated under UV. The DNA release ability was evaluated by salt separation. Complexes with an N/P ratio of 20 were prepared and incubated in 25 nM DTT at 37 °C for 2 h. Samples were analyzed with agarose gel electrophoresis under the same conditions.

5.6.3 In vitro drug release study

The pH-dependence of the drug release behavior of the Co-PMs was shown using a GloMax-Multi Jr Single Tube Mutiode Reader. To examine the pH-dependent dye release, 10% Co-PMs solution was treated with solutions of disodium hydrogen phosphate citrate buffer at different pHs (pH 5.5, and pH 7.4). The amount of DOX-EMCH released at each time point was determined by fluorescence detector analysis.

5.7 Cellular uptake assay

si-Beclin1 and DOX uptake by PC-3 cells was analyzed using flow cytometry. PC3 cells were seeded into 12-well plates at 3×10^5 cells per well and incubated for 24 h at 37℃ in 5% CO2. To determine the cellular uptake of si-Beclin1 by Co-MPs, FAM-labeled si-Beclin1(FAM-si-Beclin1) was complexed with DOX-MPs at N/P of 10, 20, 40 and 80 to obtain Co-MPs and incubated for 30 min. For DOX uptake, DOX solution and DOX-MPs were added to PC3 cells, with a final DOX concentration of 0.5 μg/mL, 1 μg/mL and 2 μg/mL. After 4-h incubation, cells were washed, trypsinized, centrifuged, re-suspended in 300 μl PBS, and finally

analyzed on a FACScan flow cytometer (Becton Dickinson, SanJose, CA, USA). The experiment was repeated 3 times.

For confocal laser scanning microscopy (CLSM), PC3 cells were seeded into glass-bottom 24-well plates at a density of 1×10^5cells per well and incubated for 24 h. After replacing the culture medium, the free DOX solution, DOX-MPs, Co-MPs were added to PC3 cells with a final FAM-1-si-Beclin1 concentration of 100 nM and a final DOX concentration of 0.5 μg/mL. After 4-h incubation, the medium was discarded, the cells were fixed using 4% paraformaldehyde and treated with 4,6-diamidino-2-pheylinole dihydrochoride to stain the nucleus. Then, the cells were washed, sealed with mounting medium, and imaged using a CLSM.

5.8 Autophagy observation

5.8.1 Flow cytometry

PC3 cells were seeded into glass-bottom 12-well plates at a density of 3×10^5cells per well and incubated for 24 h. After replacing the culture medium, the si-Beclin1, free DOX solution, DOX-MPs, Co-MPs were added to PC3 cells with a final si-Beclin1 concentration of 100 nM and a final DOX concentration of 0.5 μg/mL and incubated for 24 h. After removal of the culture medium, cells were washed twice with PBS and trypsinized. Added 1 mL of the autophagosome detection reagent working solution to each well, and incubated the cells at 37°C with 5% CO_2 for 30 min. Then, washed the cells with the Wash Buffer 3 times, and re-suspended in 300 μl PBS, and finally analyzed on a FACScan flow cytometer (Becton Dickinson, SanJose, CA, USA). The autophagosome fluorescence intensity of measurement was λex = 360/λem = 520 nm. The experiment was repeated 3 times.

5.8.2 CLSM observation

PC3 cells were transiently transfected with mRFP-EGFP-LC3 plasmid using Lipofectamine 2000 (Invitrogen, USA). After 24-h incubation, PC3 cells were treated with si-Beclin1, DOX, DOX-MPs and CO-MPs for another 24 h. Then, the mRFP-EGFP-LC3 punctate structures were observed using a confocal laser scanning microscope (Olympus, Japan).The experiment was repeated for 3 times, and more than 50 cells were calculated. The number of mREF-EGFP -LC3 punctates per cell was counted.

5.8.3 TEM

PC3 cells were seeded into glass-bottom 6-well plates at a density of 5×10^5cells per well and incubated for 24 h. After replacing the culture medium, the si-Beclin1, free DOX solution, DOX-MPs, Co-MPs were added to PC3 cells with a final si-Beclin1 concentration of 100 nM and a final DOX concentration of 0.5 μg/mL and incubated for 24 h. Then, cells were washed, trypsinized, centrifuged, and re-suspended in pro-cooling fixed liquid using a 1.5 mL tip centrifuge tubes, fixed 4–6 h at 4°C, dehydrated in increasing concentrations of ethanol and acetone, embedded in Araldite, sliced into (5–7 nanometers) sections, post-stained with uranyl acetate and lead citrate, and finally examined under a Hitachi H7650 transmission electron microscope.

5.8.4 Quantitative real-time PCR

The level of beclin1 mRNA was analyzed by reverse transcription-PCR (qRT-PCR). PC3 cells were seeded into glass-bottom 6-well plates at a density of 5×10^5cells per well and incubated for 24 h. After replacing the culture medium, the si-Beclin1, free DOX solution, DOX-MPs, Co-MPs were added to PC3 cells with a final si-Beclin1 concentration of 100 nM and a final DOX concentration of 0.5 μg/mL and incubated for 24 h. Total RNA was extracted with Trizol (Invitrogen, USA) following the protocol of the manufacture. qRT-PCR analysis was performed using Applied Biosystems 7300(Thermo Fisher, USA). All data were analyzed using GAPDH as an internal standard. Primer sequences used were as follows: LC3 (forward: 5'-GTCCTGGACAAGACCAAGTTTT-3', reverse: 5'-AGGCGTAGACCATATAGAGGAAG-3'). GAPDH (forward: 5'-ACTTTGGTATCGTGGAAGGACTCAT-3', reverse: 5'-GTTTTTCTAGACGGCAGGTCAGG-3'.

5.8.5 Western Blot assay

PC3 cells were seeded in 6-well plates at a density of 5×10^5 cells per well, and incubated for 24 h. The cells were treated with different groups for 24 h, and subsequently harvested and resuspended with RIPA lysis buffer, followed by 30-min incubation on ice. Then, the protein sample was collected. An equal amount of protein was denatured by boiling for 5 min, separated by SDS-PAGE, transferred onto PVDF membrane (Millipore, USA), and blocked using 5% nonfat dried milk at RT for 1 h, then probed with antibodies P62, Beclin1, LC3. Bands were quantified by Image J software.

5.9 Cytotoxicity assay

To evaluate the cytotoxicity of DOX and si-Beclin1, a CCK-8 assay was performed. Briefly, PC3 cells were seeded into 96-well plates at a density of 1×10^4 cells per well, and incubated for 24 h. The medium was then replaced with fresh culture medium containing various concentrations of the polymer. Cells without treatment were used as a control. After 24-h and 48-h incubation, fresh medium containing a 10% CCK-8 solution was added. The absorbance of each well was measured at 450 nm using a microplate reader (Thermo Fisher Scientific, Waltham, MA, USA). The absorbance of the untreated cells was set at 100%, and cell viability was expressed as the percentage relative to the absorbance of the untreated cells. The experiment was repeated three times.

5.10 Cell apoptosis

To determine the effect of Co-MPs on cell apoptosis, PC3 cells were seeded into 12-well plates (3×10^5 cells/well) and treated with si-Beclin1, DOX, DOX-MPs and Co-MPs (0.5 μ/mL DOX and 100 nM si-Beclin1) for 48 h. Cells without treatment were used as control. For the quantitative measurement of apoptosis, cells were harvested, washed twice with ice-cold PBS and then stained with Annexin V-FITC and PT for 15 min at room temperature in the dark. The apoptosis was analyzed by flow cytometry(FACSCalibur; BD Biosciences, UK)

5.11 Biodistribution and in vivo anti-tumor effect

The fluorescence of DOX was used to investigate the distribution of micelles in vivo. The absorbance of DOX was measured at 488 nm. A subcutaneous tumor model was generated by injection of 0.1 mL of PC3 cells suspension(1×10^6) into the right axilla of nude mice. The tumors were allowed to grow to approximately 100 m3 before the experiment. To determine the tissue distribution of DOX, 18 female nude mice bearing PC3 prostatic cancer were equally randomized to three groups and injected with DOX and DOX-MPs (5 mg/kg). The mice were sacrificed 24 h later to excise the heart, liver, spleen, lung, kidney and the tumor. The excised organs and tumors were washed with cold saline and imaged using the FX Pro in vivo imaging system (Carestream Health, USA).

An in vivo anti-tumor effect assay was carried out as follows: 30 mice bearing visible PC3 tumors were equally randomized into saline, si-Beclin1, DOX, DOX-MPs and Co-MPs groups. The mice were intravenously administered with the respective formulation daily for three days at a dose of 5 mg/kg DOX and 2 mg/kg si-Beclin1. The body weight and tumor volumes ([major axis]×[minor axis]2/2, measured by calipers) were monitored and recorded twice per week for 21 days. Then, the mice were sacrificed, and their tumors were excised, weighed and photographed. Tumor volume(V) was calculated as: $V = A \times B^2/2$.

5. 12 Tunel And Immunohistochemical Analysis

Paraffin-embedded tumor tissue sections (5 μm) were subjected to TUNEL analysis, and immunohistochemistry according to standard protocols provided by the manufacturers. Apoptotic signals in tissue sections were visualized by microscopy. Immunohistochemical analyses of LC3II/I, Ki67 and Paxillin were performed. Briefly, sections were permeabilized with incubated with the LC3, Ki67 or Paxillin antibody(Cell Signaling Technology, Danvers, MA) overnight at 4℃. After washing with PBS, samples were incubated with HRP-conjugated secondary antibody (Cell Signaling Technology, Danvers, MA). LC3, Ki67 and TUNEL-postive cells were captured with a Nikon E-800 M microscope (Tokyo, Japan).

5. 13 Histologic Analysis

After the nude mice were sacrificed, hearts, livers, spleen, lung and kidney were collected and fixed in 4% paraformaldehyde for 24 h and subsequently embedded in paraffin. Tissue sections (5μm) were subjected to H&E staining.

5.14 in vivo TEM: the tumor tissues sections (2-3mm) were subjected to observe autophagy by transmission electron microscopy. Briefly, tissues were collected and fixed with 2% glutaraldenhyde solution immediately, and fixed overnight at 4℃, dehydrated in increasing concentrations of ethanol and acetone, embedded in Araldite, sliced into (5-7 nanometers) sections, post-stained with uranyl acetate and lead citrate, and finally examined under a Hitachi H7650 transmission electron microscope.

5.15 Statistical analysis

All values are presented as the mean±SD. Each value is the mean of at least three repetitive experiments in each group. The statistical significance was determined using Student's t-test. The differences were considered significant for *p<0.05.

Declarations

Acknowledgments

We acknowledge the funding supports from the National Natural Science Foundation of China (Grants 81672516, 81672545); the Science and Technology Project of Jiaxing, Zhejiang, China(Grants 2019AY32013); and the Research Fund for Academician Lin He New Medicine(Grants 199331309).

References

1. Siegel R L, Miller K D, Jemal A. Cancer statstics, 2019[J]. CA Cancer J Clin, 2019, 69:7-34.
2. Nader R, Amm J E, Aragon-Ching J B. Role of chemotherapy in prostate cancer[J].Asian J Androl, 2018,20:221-229.
3. Blessing A M, Rajapakshe K, Bollu L R, Shi Y, White M A, Pham A H,et al. Transcriptional regulation of core autophagy and lysosomal genes by the androgen receptor promotes prostate cancer progression[J]. Autophagy, 2017, 13:506-521.
4. Cai Z H, Chen W J, Zhang J Z, Li H J. Androgen receptor: what we know and what we expect in castration-resistant prostate cancer[J]. Int Urol Nephrol, 2018, 50:1753-1764.
5. Nevedomskaya E, Baumgart S J, Haendler B. Recent Advances in Prostate Cancer Treatment and Drug Discovery[J]. Int J Mol Sci, 2018, 19:1359.
6. Quinn D I, Sandler H M, Horvath L G, Goldkorn A, Eastham J A. The evolution of chemotherapy for the treatment of prostate cancer[J]. Ann Oncol, 2017, 28:2658-2669.
7. Barata P C, Sartor A O. Metastatic castration-sensitive prostate cancer: Abiraterone, docetaxel, or…[J]. Cancer2019, 125:1777-1788.
8. Evans A J. Treatment effects in prostate cancer[J]. Mod Pathol, 2018, 31:S110-121.
9. Ramos-Esquivel A, Fernández C, Zeledón Z. Androgen-deprivation therapy plus chemotherapy in metastatic hormone-sensitive prostate cancer. A systematic review and meta-analysis of randomized clinical trials[J]. Urol Oncol, 2016, 34:335.e9-335.e19.
10. Gupta S, Gupta P K, Dharanivasan G, Verma R S. Current prospects and challenges of nanomedicine delivery in prostate cancer therapy[J]. Nanomedicine (Lond), 2017, 12:2675-2692.
11. Farrow J M, Yang J C, Evans C P. Autophagy as a modulator and target in prostate cancer[J]. Nat Rev Urol, 2014, 11:508-16.
12. Naponelli V, Modernelli A, Bettuzzi S, Rizzi F. Roles of autophagy induced by natural compounds in prostate cancer[J]. Biomed Res Int, 2015, 2015:121826.

13. Li Y J, Lei Y H, Yao N, Wang C R, Hu N, Ye W C, et al. Autophagy and multidrug resistance in cancer[J]. Chin J Cancer, 2017, 36:52.
14. Chen C, Lu L, Yan S C, Yi H M, Yao H, Wu D, et al. Autophagy and doxorubicin resistance in cancer[J]. Anticancer Drugs, 2018, 29:1-9.
15. Wirawan E, Berghe T V, Lippens S, Agostinis P, Vandenabeele P. Autophagy: for better or for worse[J]. Cell Res, 2012, 22: 43-61.
16. Yun C W, Lee S H. The Roles of Autophagy in Cancer[J]. Int J Mol Sci, 2018, 19:3466.
17. Onorati A V, Dyczynski M, Ojha R, Amaravadi R K. Targeting autophagy in cancer[J]. Cancer, 2018 , 124:3307-3318.
18. Hsieh M J, Lin C W, Yang S F, Sheu G T, Yu Y Y, Chen M K, et al. A combination of pterostilbene with autophagy inhibitors exerts efficient apoptotic characteristics in both chemosensitive and chemoresistant lung cancer cells[J]. Toxicol Sci, 2014, 137:65-75.
19. Pan B, Chen D, Huang J, Wang R, Feng B, Song H Z, et al. HMGB1-mediated autophagy promotes docetaxel resistance in human lung adenocarcinoma[J]. Mol Cancer, 2014, 13:165.
20. Jiang Y, Yang N, Zhang H, Sun B, Hou C Y, Ji C, et al. Enhanced in vivo antitumor efficacy of dual-functional peptide-modified docetaxel nanoparticles through tumor targeting and Hsp90 inhibition[J]. J Control Release, 2016, 221:26-36.
21. Rohatgi R A, Janusis J, Leonard D, BellvéK D , Fogarty K E, Baehrecke E H, et al. Beclin 1 regulates growth factor receptor signaling in breast cancer[J]. Oncogene, 2015, 34: 5352-5362.
22. Liang X H, Jackson S, Seaman M, Brown K , Kempkes B , Hibshoosh H, et al. Induction of autophagy and inhibition of tumorigenesis by beclin 1[J]. Nature, 1999, 402: 672-676.
23. Russo M, Russo GL. Autophagy inducers in cancer[J]. Biochem Pharmacol, 2018. 153:51-61.
24. De S, Das S, Sengupta S. Involvement of HuR in the serum starvation induced autophagy through regulation of Beclin1 in breast cancer cell-line, MCF-7[J]. Cell Signal, 2019, 61:78-85.
25. Yang M, Yang X M, Yin D H, Tang Q L, Wang L,, Huang C, et al. Beclin1 enhances cisplatin-induced apoptosis via Bcl-2-modulated autophagy in laryngeal carcinoma cells Hep-2[J]. Neoplasma, 2018, 65:42-48.
26. 26.Aita V M, Liang X H, Murty V, Pincus D L, Yu W , Cayanis E, et al. Cloning and genomic organization of beclin 1, a candidate tumor suppressor gene on chromosome 17q21[J]. Genomics, 1999, 59: 59-65.
27. Xi G, Hu X, Wu B, Jiang H M, Young C Y F, Pang Y X. Autophagy inhibition promotes paclitaxel-induced apoptosis in cancer cells[J]. Cancer lett, 2011, 307: 141-148.
28. Saleem A, Dvorzhinski D, Santanam U, Mathew R, Stein M, White E, et al. Effect of dual inhibition of apoptosis and autophagy in prostate cancer[J]. Prostate, 2012, 72: 1374-1381.
29. Futaki S, Suzuki T, Ohashi W, Yagami T , Tanaka S , Ueda K, et al. Arginine-rich peptides An abundant source of membrane-permeable peptides having potential as carriers for intracellular protein delivery[J]. J BiolChem, 2001, 276: 5836-5840.

30. Futaki S. Membrane-permeable arginine-rich peptides and the translocation mechanisms[J]. Adv Drug Deliver Rev, 2005, 57: 547-558.
31. Lorents A, Säälik P, Langel Ü, Pooga M. Arginine-Rich Cell-Penetrating Peptides Require Nucleolin and Cholesterol-Poor Subdomains for Translocation across Membranes[J]. Bioconjug Chem, 2018, 29:1168-1177.
32. Lächelt U, Kos P, Mickler F M, Herrmann A, Salcher E E, Rödl W, et al. Fine-tuning of proton sponges by precise diaminoethanes and histidines in pDNA polyplexes[J]. Nanomedicine, 2014, 10:35-44.
33. Midoux P, Pichon C, Yaouanc J J, JaffrèsP A. Chemical vectors for gene delivery: a current review on polymers, peptides and lipids containing histidine or imidazole as nucleic acids carriers[J]. Br J Pharmacol, 2009, 157:166-78.
34. Yin J, Ren W, Yang G, Duan J L , Huang X G , Fang R J, et al. L-Cysteine metabolism and its nutritional implications[J]. Mol Nutr Food Res, 2016, 60:134-46.
35. Tian M, Guo F, Sun Y, Zhang W J , Miao F , Liu Y, et al. A fluorescent probe for intracellular cysteine overcoming the interference by glutathione[J]. Mol Nutr Food Res, 2016, 60:134-46.
36. Acharya S, Sahoo SK. PLGA nanoparticles containing various anticancer agents and tumour delivery by EPR effect[J]. Adv Drug Deliv Rev, 2011, 63:170-183.
37. Conner SD, Schmid SL. Regulated portals of entry into the cell[J]. Nature, 2003, 422: 37-44.
38. Derakhshankhah H, Jafari S. Cell penetrating peptides: A concise review with emphasis on biomedical applications[J]. Biomed Pharmacother, 2018, 108:1090-1096.
39. Jafarzadeh-Holagh S, Hashemi-Najafabadi S, Shaki H, Vasheghani-Farahani E. Self-assembled and pH-sensitive mixed micelles as an intracellular doxorubicin delivery system[J]. J Colloid Interface Sci, 2018, 1, 523: 179-190.
40. Du C, Liang Y, Ma Q, Sun Q W, Qi J H , Cao J, et al. Intracellular tracking of drug release from pH-sensitive polymeric nanoparticles via FRET for synergistic chemo-photodynamic therapy[J]. J Nanobiotechnology, 2019, 7, 17:113.
41. Li Z, Qiu L, Chen Q, Hao T N , Qiao M X , Zhao H X, et al. pH-sensitive nanoparticles of poly(L-histidine)-poly(lactide-co-glycolide)-tocopheryl polyethylene glycol succinate for anti-tumor drug delivery[J]. Acta Biomater, 2015, 11:137-150.
42. Yameen B, Choi WI, Vilos C, Swami A, Shi J J, Farokhzed O C. Insight into nanoparticle cellular uptake and intracellular targeting[J]. J Control Release, 2014, 190:485-99.
43. Tai Z, Wang X, Tian J, Gao Y , Zhang L J , Yao C, et al. Biodegradable Stearylated Peptide with Internal Disulfide Bonds for Efficient Delivery of siRNA In Vitro and In Vivo. Biomacromolecules, 2015, 16:1119–1130.
44. Ross N L, Munsell E V, Sabanayagam C, Sullivan M O. Histone-targeted Polyplexes Avoid Endosomal Escape and Enter the Nucleus During Postmitotic Redistribution of ER Membranes[J]. Mol Ther Nucleic Acids, 2015, 4:e226.

45. Zhou C, Zhong W, Zhou J, Sheng F F , Fang Z Y , Wei Y, et al. Monitoring autophagic flux by an improved tandem fluorescent-tagged LC3 (mTagRFP-mWasabi-LC3) reveals that high-dose rapamycin impairs autophagic flux in cancer cells[J]. Autophagy, 2012, 8:1215-26.
46. Yoshii SR, Mizushima N. Monitoring and Measuring Autophagy[J]. Int J Mol Sci, 2017, 28, 18:1865.
47. 47.Feng Q, Yu M Z, Wang J C, Hou W J , Gao L Y, Ma X F, et al. Synergistic inhibition of breast cancer by co-delivery of VEGF siRNA and paclitaxel via vapreotide-modified core–shell nanoparticles, Biomaterials, 2014, 35:5028–5038.
48. Gomari H, Forouzandeh Moghadam M, Ghavami M, Khodashenas S. Targeted delivery of doxorubicin to HER2 positive tumor models[J]. Int J Nanomedicine, 2019, 14:5679-5690.
49. Qian F, Stowe N, Liu E H, Saidel G M, Gao J M. Quantification of in vivo doxorubicin transport from PLGA millirods in thermoablated rat livers[J]. J Control Release, 2003, 91:157-66.
50. Maeda H, Nakamura H, Fang J. The EPR effect for macromolecular drug delivery to solid tumors: Improvement of tumor uptake, lowering of systemic toxicity, and distinct tumor imaging in vivo[J]. Adv Drug Deliv Rev, 2013, 65:71-79.
51. Maeda H. Polymer therapeutics and the EPR effect[J]. J Drug Target Nov-Dec, 2017, 25:781-785.
52. Lv S X, Tang Z H, Li Z Q, Lin J, Song W T, Liu H Y, et al. Co-delivery of doxorubicin and paclitaxel by PEG-polypeptide nanovehicle for the treatment of non-small cell lung cancer[J]. Biomaterials, 2014, 35:6118-6129.
53. Li X R, Yang X C, Lin Z Q, Wang D, Mei D, He B, et al. A folate modified pH sensitive targeted polymeric micelle alleviated systemic toxicity of doxorubicin (DOX) in multi-drug resistant tumor bearing mice[J]. Eur J Pharm Sci, 2015, 76:95-101.
54. Jiang Y, Yang N, Zhang H F, Sun B, Hou C Y, Ji C, et al. Enhanced in vivo antitumor efficacy of dual-functional peptide-modified docetaxel nanoparticles through tumor targeting and Hsp90 inhibition[J]. J Control Release, 2016, 221:26-36.
55. Zhang X D, Yang Y, Liang X, Zeng X W, Liu Z G, Ta**o** W, et al. Enhancing Therapeutic Effects of Docetaxel-Loaded Dendritic Copolymer Nanoparticles by Co-Treatment with Autophagy Inhibitor on Breast Cancer[J]. Theranostics, 2014, 4:1085-1095.
56. Mathew R, Kongara S□Beaudoin B□Karp C M□Bray K□Degenhardt K, et al. Autophagy suppresses tumor progression by limiting chromosomal instability[J]. Genes Dev, 2007, 21:1367-1381.

Figures

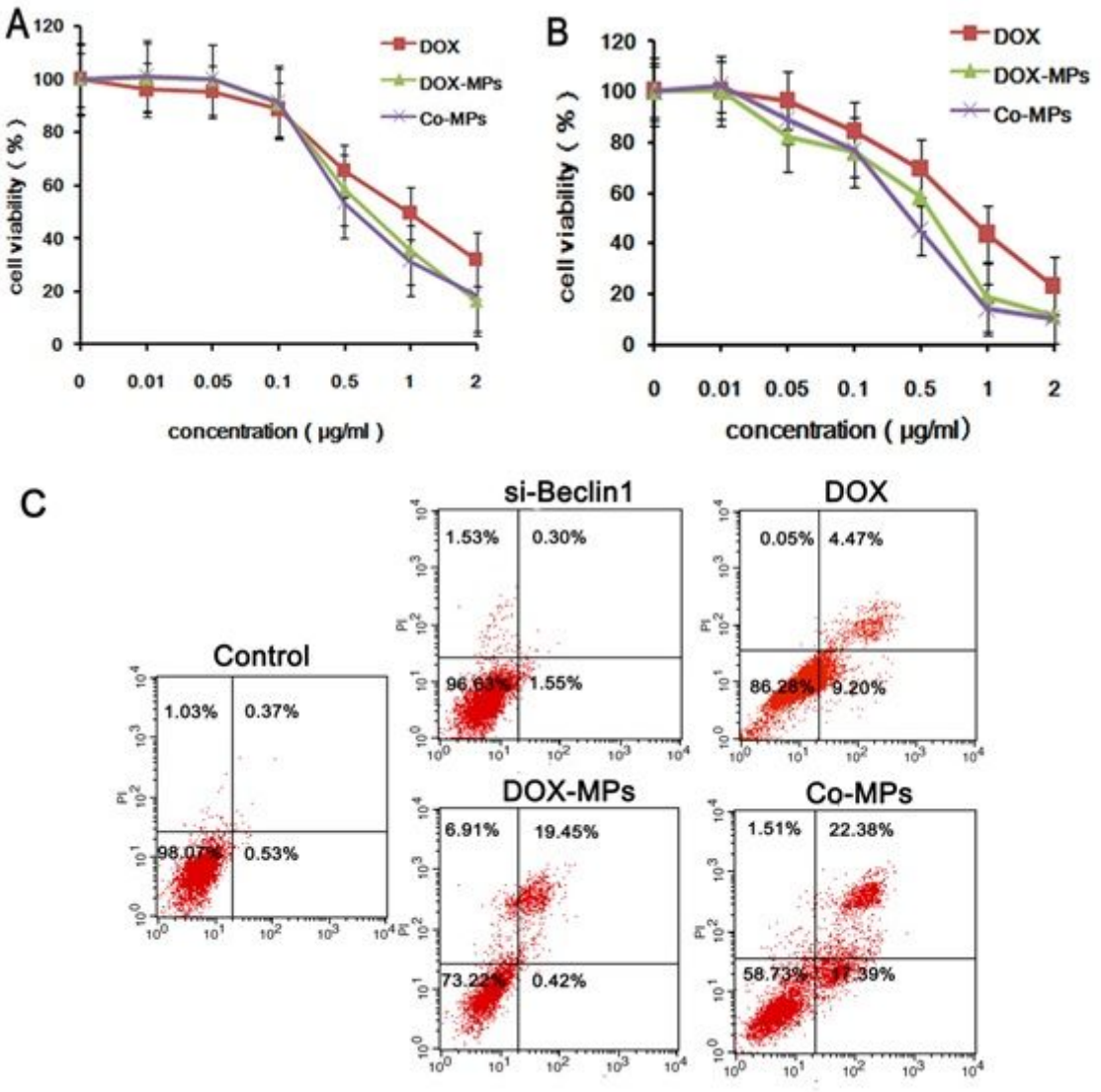

Figure 1

In vitro anti-tumor effect of Co-MPs. (A) Viability of PC3 cells after treatment with DOX, DOX-MPs and Co-MPs at different DOX concentrations for 24h. (B) Viability of PC3 cells after treatment with DOX, DOX-MPs and Co-MPs at different DOX concentrationsfor 48h. (C) Cell apoptotic assay. Cell apoptosis analysis of PC3 cells treated by different formulations for 48 h and measured by flow cytometry using annexin V-APC kit and PI staining. The concentration of DOX and si-Beclin1 was 0.5 μg/mL and 100 nM. Data are expressed as the mean ± SD (n = 3).

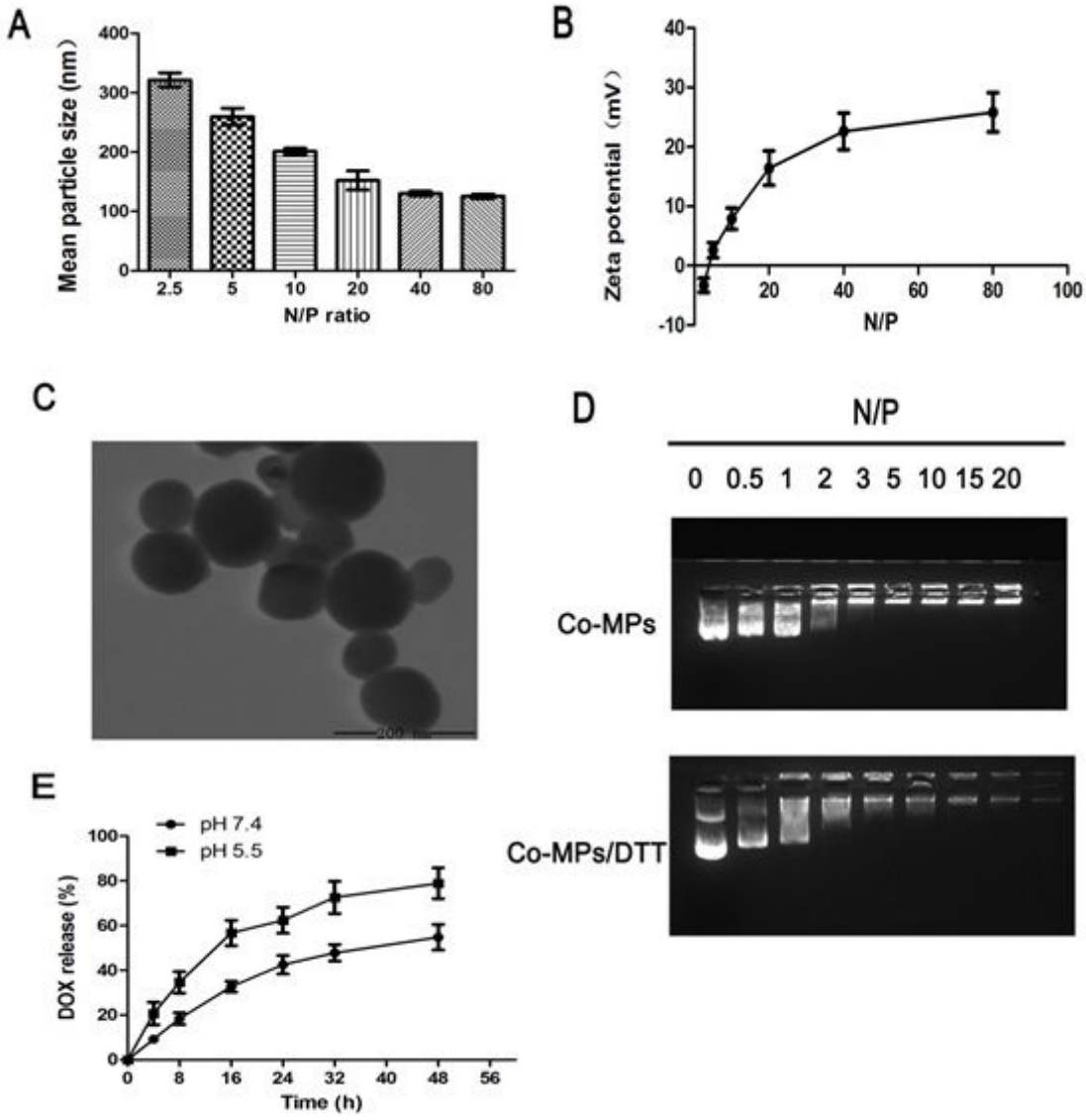

Figure 1

Characterization of Co-MPs.(A) Particle size of Co-MPs determined by DLS. (B) Zeta potential of Co-MPs determined by DLS. (C) TEM images of Co-MPs at a N/P ratio of 40. (D) Agarose electrophoresis result of Co-MPs. (E) Profiles of DOX release from Co-PMs in PBS at pH 5.5 and pH 7.4 at 37 °C.

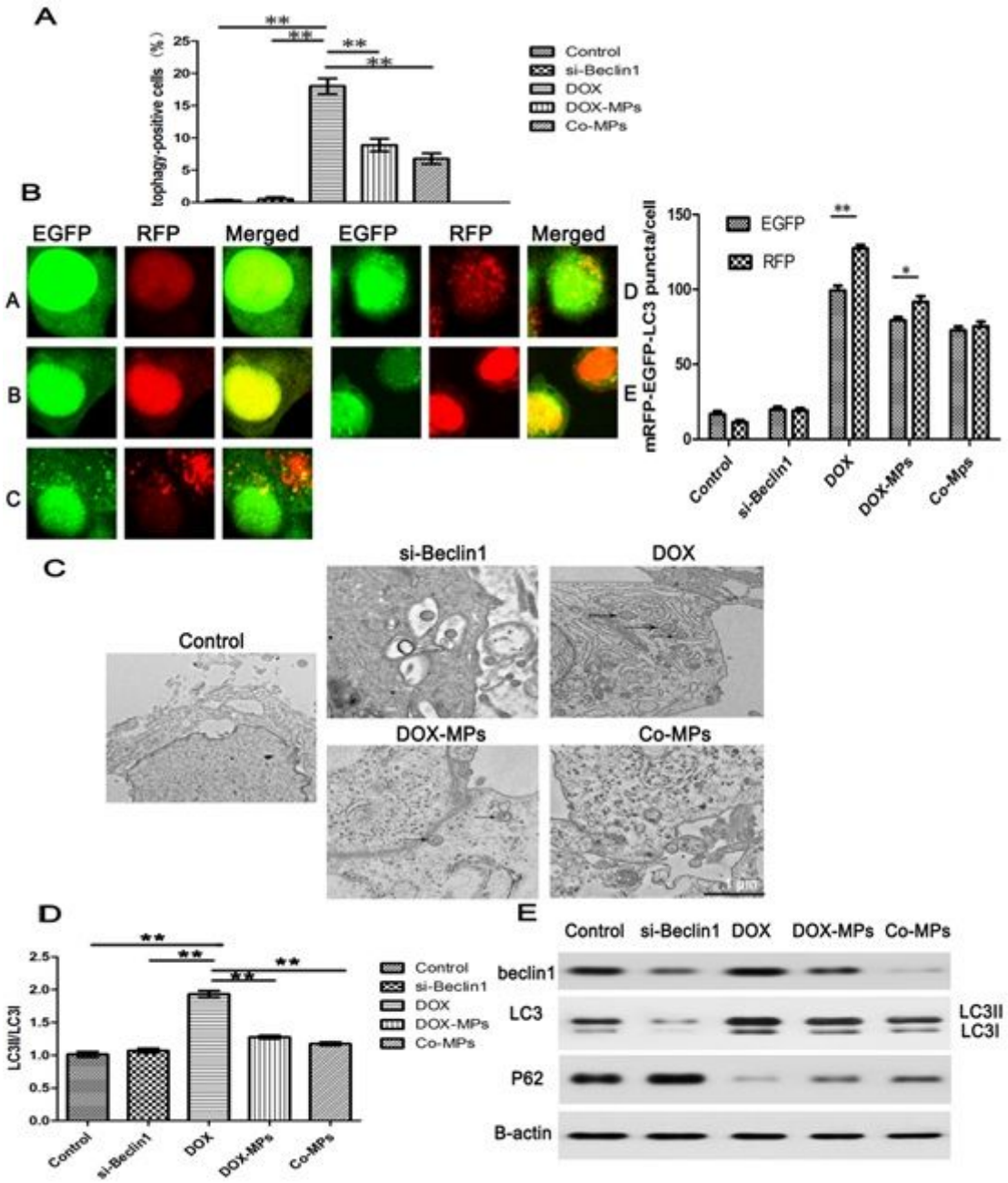

Figure 1

Autophagy assay. (A) Quantitative analysis of the percentages of positive autophagy cells of PC3 cells treated with si-Beclin1, DOX, DOX-MPs and Co-MPs. The Concentration of DOX and si-Beclin1was 0.5 μg/mL and 100 nM for 24 h. Data are expressed as the mean ± SD (n = 3). (B) PC3 cells stably expressing mRFP-EGFP-LC3 were treated with si-Beclin1, DOX, DOX-MPs and Co-MPs for 24 h. The formation of puncta was imaged using a confocal microscope and representative images are presented. The number of EGFP-LC3 and REF-LC3 puncta per cell was calculated. For quantification, at least 20 cells per experiment were randomly selected for counting the number of mRFP-LC3 or EGFR-LC3 puncta in each treatment group. Data are presented from one representative experiment of three independent experiments. *p < 0.05, **p < 0.01. (C) transmission electron microscopy images of PC3 cells following si-

Beclin1, DOX, DOX-MPs and Co-MPs (DOX: 0.5 μg/mL, 100 nM si-Beclin1) for 24 h. Scale bar is 1 μm. (D) qRT-PCR quantification of LC3II/I protein expressed in PC3 cells. (D) Western blot analysis of Beclin1, LC3 and p62 protein levels in PC3 cells.Data are presented from one representative experiment of three independent experiments. *p < 0.05, **p < 0.01.

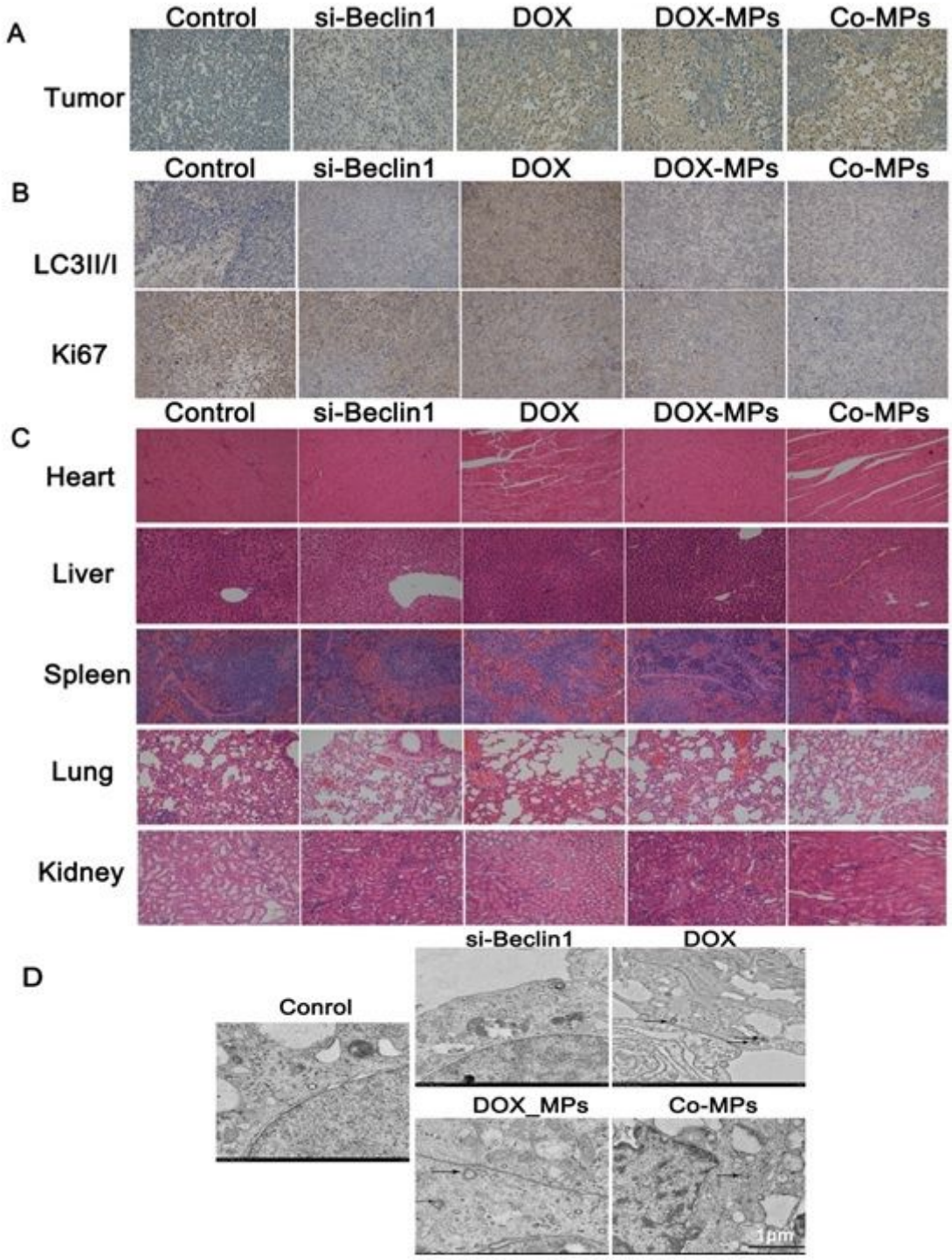

Figure 1

(A) TUNEL-staining of tumor tissue(200X). (B) Immunohistochemistry to detect LC3 and Ki67 in tumors. The images were acquired with a Leica microsCope at low magnification (200X). (C) The histological

characteristics of PC3 tumor tissue and organ histology after treatment with PBS, si-Beclin1, DOX, DOX-MPs and Co-MPs. (D) transmission electron microscopy images of PC3 tumor following si-Beclin1, DOX, DOX-MPs and Co-MPs. Scale bar is 1 μm.

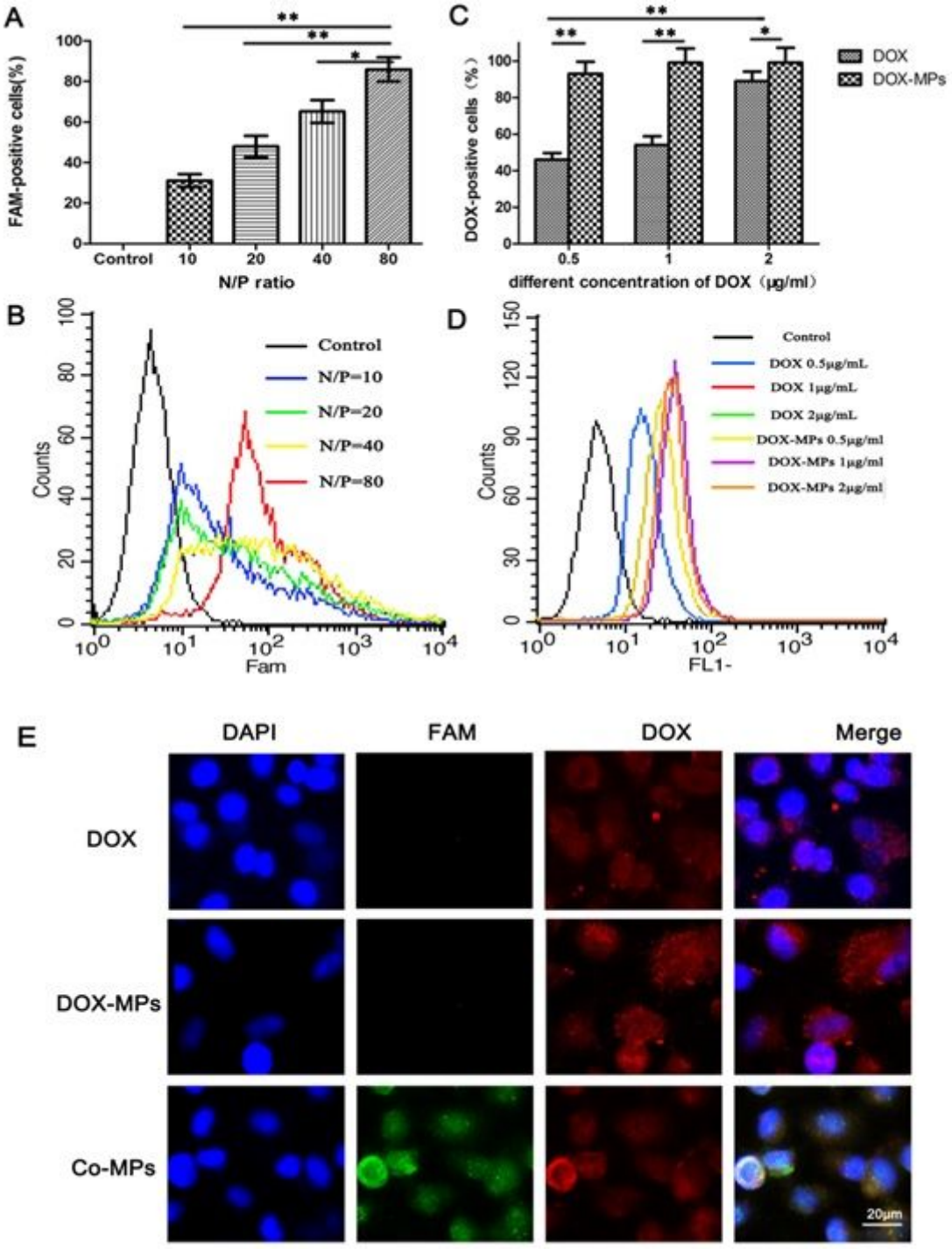

Figure 1

Cellular uptake of DOX and FAM-si-Beclin1. (A) Quantitative analysis of FAM-si-Beclin1 uptake in PC3 cells after Co-MPs treatment for 4h at different N/P ratios. (B) Flow cytometry figures display FAM expression of PC3 cells after treatment with Co-MPs at different N/P ratios. (C) Quantitative analysis of DOX uptake in PC3 cells after 4-h treatment with DOX and DOX-MPs at different concentrations of DOX.

(D) Flow cytometry figures display DOX uptake of PC3 cells after treatment with DOX and DOX-MPs at different DOX concentrations.(E) Confocal microsCopic images of PC3 cells incubated with DOX(a), DOX-MPs(b) and Co-MPs(c) for 4 h. Green signal represent FAM-labeled si-Beclin1, red signals represent DOX and blue signals represent the cell nucleus. Scale bar is 20 μm.

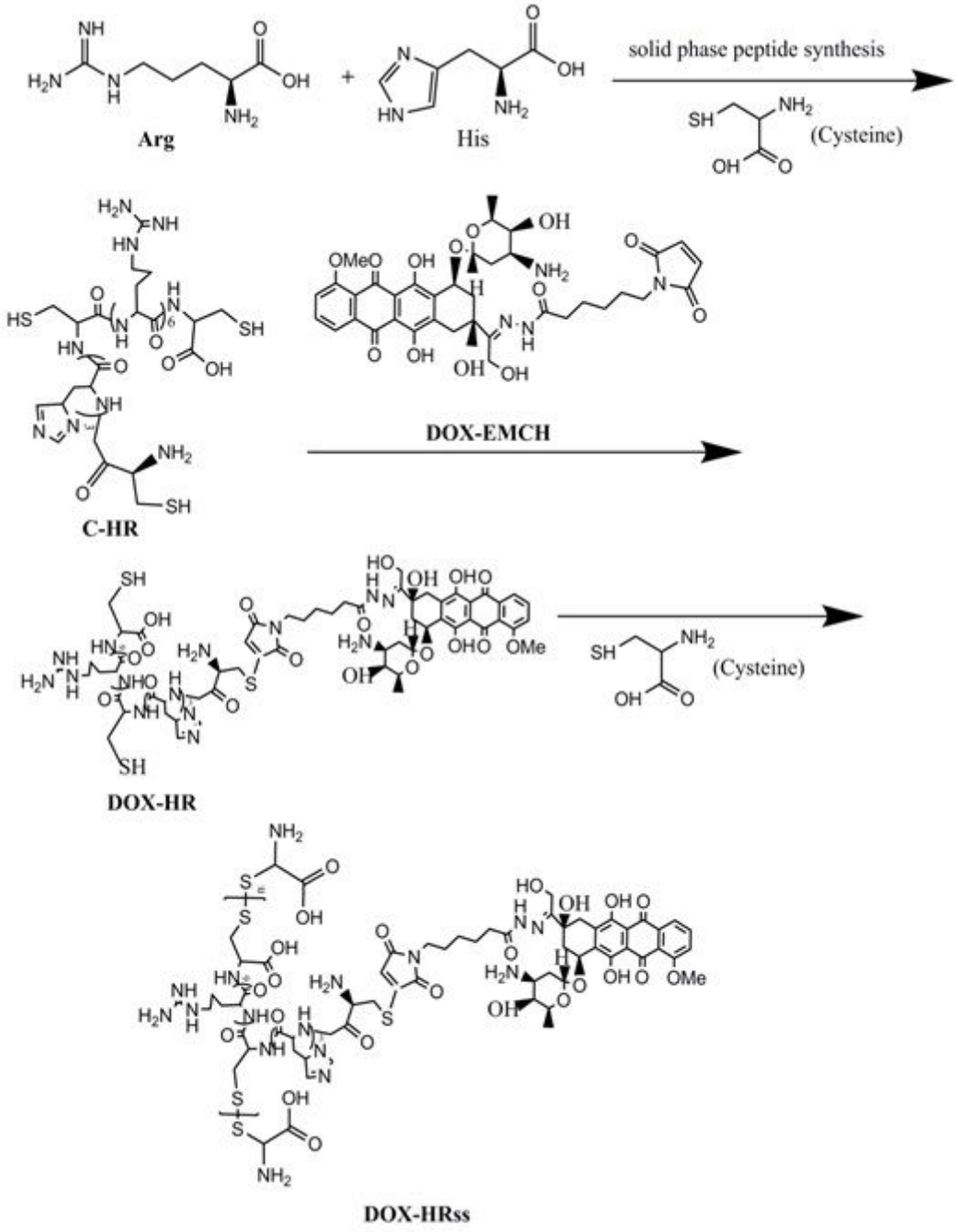

Figure 1

The structure, drug loading process and intracellular uptake of poly(L-arginine)-poly(L-histidine)-DOXO-EMCH

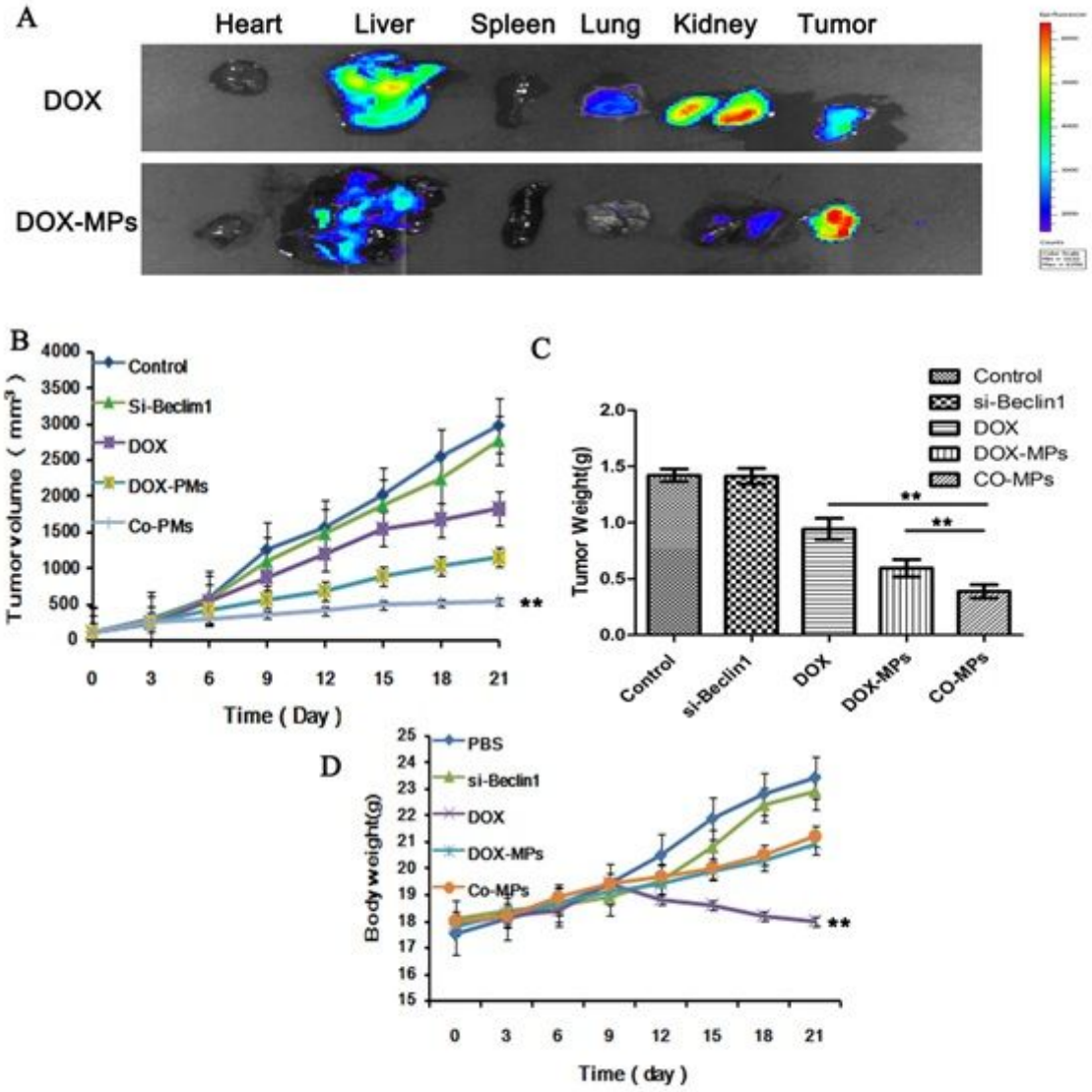

Figure 1

(A) Ex vivo imaging of tumors and organs collected at administered DOX, DOX-MPs and for 24h(DOX: 0.5 μg/mL, 100 nM si-Beclin1). (B) In vivo efficacy evaluation of Co-MPs through i.v. injection in PC3 xenografts tumor-bearing nude mice. Tumor growth curve of mice treated with PBS, si-Beclin1, DOX, DOX-MPs and Co-MPs. (C) The weight of the excised tumor tissues fromall groups. Data are expressed as mean±SD (n=6). (D) Body weights of tumor-bearing mice treated with PBS, si-Beclin1, DOX, DOX-MPs and Co-MPs. Data are given as the mean±SD(n=6). (**p□0.01, vs PBS).

Supplementary Files

This is a list of supplementary files associated with this preprint. Click to download.

- Scheme1.jpg